

Figure S1. Immunization regimens for the three NHP studies (Related to Fig. 1)

Regimens for (A) NHP #36 (B) NHP #54 and (C) NHP #62.1. Immunogens are listed in angled boxes above black horizontal arrows and corresponding times of immunization are listed below. Time of antibody isolation is indicated by a red box and line.

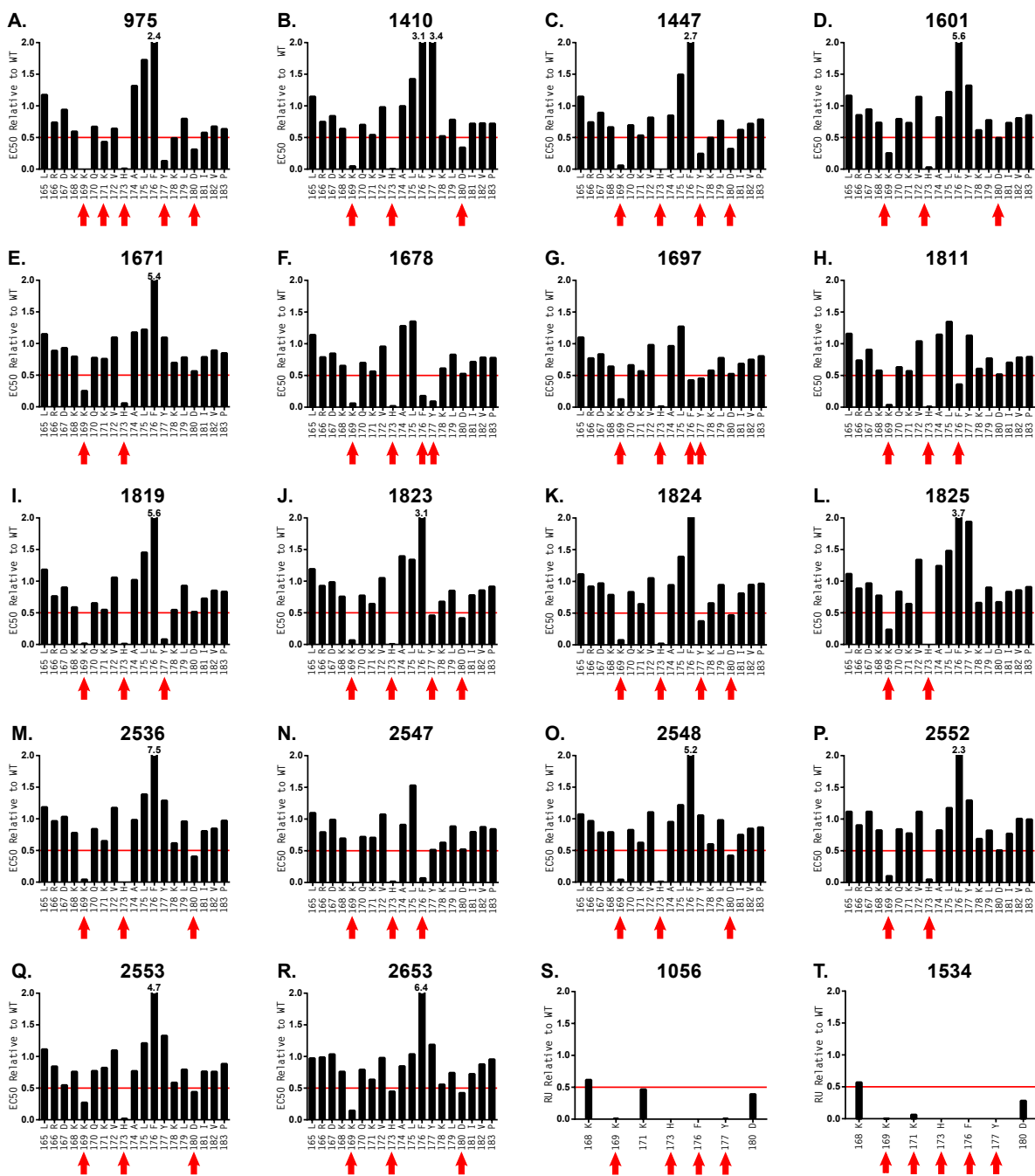


Figure S2. Epitope mapping of purified V2 antibodies (related to Table 1)

Purified antibodies were epitope mapped by alanine scanning mutations on the 171 V2 peptide. Red arrows indicate >50% reduction in binding (red line) of alanine scanning mutation at specified position relative to wild type peptide binding as measured by ELISA (EC50) (panels A-R) or SPR (Response Units) (panels S-T). Values listed are averages of measurements run in duplicate. For ease of comparison, scale of y-axis is set at 2.0 with values >2 listed above bars.

Species	AA/Codon
<i>Homo sapiens</i>	50 51 E D gag gac
<i>Pan troglodytes</i>	E D gag gac
<i>Pan paniscus</i>	E D gag gac
<i>Gorilla gorilla</i>	E D gag gac
<i>Pongo abelii</i>	K D aag gac
<i>Nomascus leucogenys</i>	E D gag gac
<i>Papio anubis</i>	E D gag gac
<i>Macaca mulatta</i>	E D gag gac
<i>Callithrix jacchus</i>	E D gaa gac
<i>Saimiri boliviensis</i>	Q D caa gat
<i>Tarsius syrichta</i>	E D gaa gat
<i>Microcebus murinus</i>	E D gag gat
<i>Otolemur garnetti</i>	E D gaa gat

Figure S3. Codon usage in ED motif in IGLV3-10 primate orthologs (Related to Fig. 5)

The use of synonymous codons in primate orthologs of human IGLV3-10 encoding glutamic acid and aspartic acid (ED) at positions 50 and 51 suggests evidence of selective pressure for maintenance of LCDR2 ED motif in the primate lineage. Amino acids (uppercase) and DNA codons (lowercase) that differ from human are shown in red.

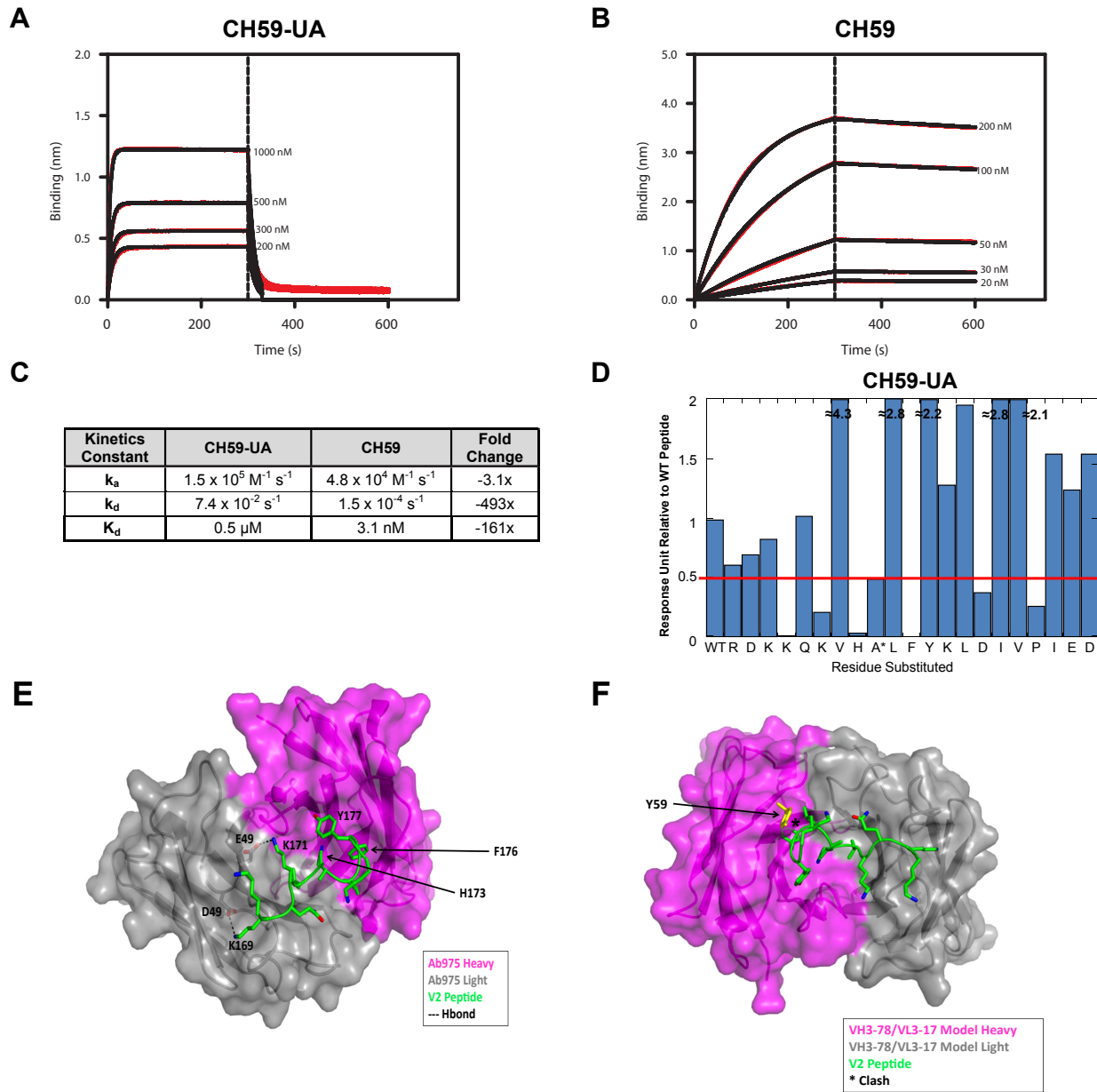


Figure S4. Structural models and binding kinetics of CH59-UA (Related to Fig. 6)

Representative bio-layer interferometry sensograms (red) and the best fit (black) are shown for the binding between wild type 171 V2 peptide and (A) CH59-UA and (B) CH59. (C) The binding kinetics parameters of CH59-UA and CH59 interactions with wild type 171 peptide are compared. The on-rate (k_a), off-rate (k_d) and dissociation constant (K_d) values were obtained by global fitting of specific binding sensograms to a 1:1 binding model and values listed are averages of triplicate measurements. (D) Epitope mapping of CH59-UA carried out using SPR measurements of alanine scans of AE.A244 gp120166-186 peptide binding of CH59-UA. Red line denotes 50% reduction in binding relative to WT peptide. Asterisk denotes alanine to glutamine mutation. To focus on epitope positions where binding decreased, the scale of y-axis is set at 2.0 with values >2 listed next to bars. Structural models of complexes of V2 peptide (green) and (E) rhesus antibody 975 and (F) a rhesus antibody with an unmutated IGHV3-78/IGLV3-17 pairing. In each model, the heavy chain (magenta) and light chain (gray) are shown in cartoon representation with a transparent surface overlaid to illustrate binding site shape. Predicted salt bridge interactions of the ED motif are shown by dashed black lines. The predicted steric clash between residue Y59 (yellow, stick representation) in the HCDR2 of IGHV3-78 and the V2 peptide is denoted by an asterisk.

A

VL	Ab/Gene	Amino Acid Sequence
IGLV3-10	CH59	SYELTQEPSSVSPGOTARITCSDGALPKNYAWYQQKSGQAFVITYEDSKRPSGIPERTSGSSGGTMAHTLISGAQVEDEADYYCYSTDDSSGNHRYFGGGTTKLTVL
IGLV3-10	CH59_UA	-----K-----
IGLV3-10	VL gene	-----K-----
IGLV3-17	VL gene	-----K-----
IGLV3-17	1678	-----F...P...S...I...ED-----
IGLV3-17	1685	-----F...P...S...I...ED-----
IGLV3-17	1687	-----F...P...S...G...I...ED-----
IGLV3-17	1803	-----F...P...S...I...FED-----
IGLV3-17	1811	-----K.V...F...P...S...I...EDP-----
IGLV3-17	1814	-----F...S...I...EDN-----
IGLV3-17	1869	-----EK...F...K...P...S...I...EDN-----
IGLV3-17	1912	-----EK...F...P...S...I...EDN-----
IGLV3-17	2562	-----EK...FH...P...S...I...EDN-----
IGLV3-17	1410	-----K.T...F...P...S...A...I...EDT-----
IGLV3-17	1816	-----K.G...F...P...S...I...EDN-----
IGLV3-17	1825	-----K...F...P...S...I...ED-----
IGLV3-17	2630	-----K...F...P...S...I...ED-----
IGLV3-17	1601	-----EK...F...P...S...I...ED-----
IGLV3-17	1671	-----EKF...F...P...S...I...ED-----
IGLV3-17	2212	-----K...F...T...S.A...IV...ED...F...X...V...V...V...F...-----
IGLV3-17	2553	-----EK...F...P...S...I...ED...R...-----
IGLV3-17	975	-----EK...F...P...S...I...EDN-----
IGLV3-17	1447	-----EK...F...P...S...I...EDN-----
IGLV3-17	1819	-----D...-----
IGLV3-17	1823	-----K...F...P...S...I...EDN-----
IGLV3-17	1824	-----EK...F...P...S...T...EDT-----
IGLV3-17	2201	-----T...EK...F...A...S...I...EDN-----
IGLV3-17	2536	-----TK...F...P...S...I...ED...R...P...-----
IGLV3-17	2547	-----M...-----
IGLV3-17	2653	-----EKF...F...P...S...I...EDN-----
IGLV3-17	2548	-----EK...F...K...P...S...I...EDN-----

B

Species	VH	Ab/Gene	Amino Acid Sequence													
human	IgHV3-9	CH59	EVQLVESGGGLVQFGRSLRLSS2ASGFTF-DDGAM-HWVRDAPGKGLEWYSGISWNSNTIAYADSUVKGERTFISRDNAKNSLYLEMNSLRVETALYYCAR D SPR--GELPLNLYWQGQTIVTVSS
human	IgHV3-9	CH59_UA	EVQLVESGGGLVQFGRSLRLSS2ASGFTF-SSYYWM-NWROTGPGRKLEWYSGISWNSNTIAYADSUVKGERTFISRDNAKNSLYLEMNSLRVETALYYCAR D SPR--GELPLNLYWQGQTIVTVSS
rhesus	IgHV3-SC11	1678	EVOLVESGGGLAKPGGSURLSLCAVSGFTF-SYYWM-NWROTGPGRKLEWYSGISWNSNTIAYADSUVKGERTFISRDNAKNSLYLEMNSLRVETALYYCAR D SPR--GELPLNLYWQGQTIVTVSS
rhesus	IgHV3-SC11	1695	D.H.....V.R.S.....DSV.H.....R...VA.FR.-.K.F.....F.S...E.....IA.....TE D
rhesus	IgHV3-SC11	1697	Q.....N.LF.H.....S.....V.F.RA.....V.GR.-.V.F.RA.....V.F.RT.-.K.F.....F.S...E.....IA.....EDG...
rhesus	IgHV3-SC11	1803	D.H.....V.R.S.....DSV.H.....R...VA.FR.....V.YB.FRT.-.K.F.....F.E.....P...F.....IA.....EDG...
rhesus	IgHV3-SC11	1811	D.....V.R.S.....NSA.H.....R...VA.FSP.....F.T.....I.R..TS.E.....TD.....EDG...
rhesus	IgHV4-48	1614	QVQLQESGGFLVKPSETSLTCAVSGGSI-SS-YYNNWIRPPGKGLEWYIGGSSGTYNNPSLKSRSVTISRDTSKNQFLKLSSVTAAATAVYYCAR D SMGV.EQLPLIVWGPGLVTVSS
rhesus	IgHV4-48	1669
rhesus	IgHV4-48	1912
rhesus	IgHV4-48	2552
rhesus	IgHV4-48	1410
rhesus	IgHV4-48	1816
rhesus	IgHV4-48	1825
rhesus	IgHV4-48	2630
rhesus	IgHV4-79	1601	QVQLQESGGFLVKPSETSLTCAVSGGSI-SS-GYGNWSIROPPGKGLEWYIGGSSGTYNNPSLKSRSVTISRDTSKNQFLKLSSVTAAATAVYYCAR D SMGV.EQLPLIVWGPGLVTVSS
rhesus	IgHV4-79	1671
rhesus	IgHV4-79	1722
rhesus	IgHV4-79	2553
rhesus	IgHV4-79	975
rhesus	IgHV4-79	1447
rhesus	IgHV4-79	1819
rhesus	IgHV4-79	1823
rhesus	IgHV4-79	1824
rhesus	IgHV4-96	1701	QVQLQESGGFLVKPSETSLTCAVSGGSI-SDYYNNWIROPPGKGLEWYIGGSSGTYNNPSLKSRSVTISRDTSKNQFLKLSSVTAAATAVYYCAR D SMGV.EQLPLIVWGPGLVTVSS
rhesus	IgHV4-96	2201
rhesus	IgHV4-96	2536
rhesus	IgHV4-96	2547
rhesus	IgHV4-96	2653
rhesus	IgHV4-96	2548

Figure S5. Multiple sequence alignments of rhesus antibodies using the IgLV3-17 gene segment (Related to Fig. 3)

Multiple sequence alignments for antibody (A) light chain amino acid sequences and (B) heavy chain amino acid sequences. Dots denote matches to reference sequence (gray fill). CDRs are shaded light blue and the LCDR2 ED motif (red) has been bolded for emphasis.

Table S1. ELISA Binding Data for V2-reactive Rhesus Antibodies, Unmutated Common Ancestors and ED Motif Alanine Mutations (Related to Fig 3)

A.

mAb ID	Contains CDRL2 ED Motif?	Transient Transfection			Purified mAb
		AE A244 V1V2 Tags (OD)	A244 V2 Peptide (OD)	K169A:WT Ratio (AUC rel to WT A244 V2 Peptide)	
975	Yes	3.561	3.522	0.084	0.000
1410	Yes	3.560	3.659	0.159	0.046
1447	Yes	3.499	0.351	0.220	0.057
1601	Yes	3.599	1.899	0.296	0.253
1671	Yes	3.664	3.341	0.223	0.251
1678	Yes	3.632	3.284	0.252	0.059
1697	Yes	3.570	3.387	0.366	0.124
1811	Yes	3.584	3.214	0.119	0.037
1819	Yes	3.816	3.515	0.096	0.015
1823	Yes	3.937	3.619	0.230	0.066
1824	Yes	3.560	2.577	0.159	0.074
1825	Yes	3.398	2.857	0.975	0.235
2536	Yes	3.501	3.230	0.104	0.041
2547	Yes	3.521	3.201	0.050	0.000
2548	Yes	3.536	3.177	0.077	0.040
2552	Yes	3.663	3.596	0.267	0.101
2553	Yes	3.657	3.608	0.415	0.271
2653	Yes	3.658	3.672	0.277	0.144
1614	Yes	3.670	3.388	0.416	N/A
1669	Yes	3.608	3.389	0.182	N/A
1695	Yes	3.561	3.226	0.165	N/A
1803	Yes	3.635	3.310	0.135	N/A
1816	Yes	3.937	3.532	0.281	N/A
1912	Yes	3.557	3.310	0.410	N/A
2201	Yes	3.502	3.174	0.057	N/A
2212	Yes	3.538	3.317	0.354	N/A
2630	Yes	3.937	3.367	0.497	N/A
1510	No	3.480	1.182	0.985	N/A
1806	No	3.557	3.145	0.862	N/A
1809	No	3.561	3.179	0.822	N/A
1918	No	3.600	3.290	0.937	N/A
2090	No	3.937	3.416	0.833	N/A
2102	No	3.937	2.676	0.899	N/A
2550	No	3.744	2.876	0.610	N/A
2551	No	3.206	0.800	1.083	N/A
2554	No	3.628	3.685	0.958	N/A
2840	No	3.647	3.369	0.773	N/A
2847	No	3.548	3.377	0.944	N/A
2857	No	3.709	3.246	0.785	N/A

39 rhesus antibodies were classified as V2-reactive if OD for binding to AE.A244 V1V2 tags protein was >1 and OD to the AE.A244 V2 peptide (LRDKKQKVHALFYKLDIVPIED) was >0.3. Antibody recognition of K169 (highlighted in yellow) was established if K169A mutation resulted in >50% reduction in binding relative to wildtype AE.A244 V2 171 peptide (expressed here by a K169A:WT ratio <0.5) for either transiently transfected antibody (as measured by AUC of ODs at three concentrations) or as purified antibody (as measured by EC50).

B.

Antibody	EC50 (ug/ml)		
	A244 gp120	V1V2 Tags	V2 Peptide
1518	0.009	0.011	0.747
1518 D51A	0.093	0.023	3.299
1518 E50A+D51A	0.479	0.109	21.265

C.

Clone # ¹	Members	V1V2 Tags EC50 (ug/ml)			
		VH	VL	UCA	Mutated ²
1	1678, 1697, 1811	VH3-SC11	Vλ3-17	0.003	0.005
5	1825, 2630	VH4-48	Vλ3-17	6.713	0.006
15	2653, 2548	VH4-96	Vλ3-17	48.132	0.008

¹ See Table S2 for corresponding clone numbers² Values represent min EC50 of clonal members

Table S2. Characteristics of All V2 Antibodies in Study (Related to Fig. 1)

mAb ID	NHP Study	Animal Number	Iso-type	Clone #	HEAVY				LIGHT				
					VH	JH	heavy mut freq ¹	HCDR3 length	VL	JL	light mut freq ¹	LCDR3 Length	LCDR2 Sequence
1678	36	RhM22-11	G	1	IGHV3-SC11	IGHJ4-4	16.5%	12	IGLV3-17	IGLJ1-LC1	2.6%	11	IIYEDSK
1697	36	RhM22-11	G	1	IGHV3-SC11	IGHJ4-4	16.5%	12	IGLV3-17	IGLJ1-LC1	3.8%	11	IIYEDTK
1811	36	RhM22-11	G	1	IGHV3-SC11	IGHJ4-4	16.5%	12	IGLV3-17	IGLJ1-LC1	4.5%	11	IIYEDTR
1695	36	RhM22-11	G	2	IGHV3-SC11	IGHJ4-4	11.4%	14	IGLV3-17	IGLJ1-LC1	4.5%	11	IIYEDTK
1803	36	RhM22-11	A	2	IGHV3-SC11	IGHJ4-4	10.7%	14	IGLV3-17	IGLJ1-LC1	4.5%	11	IIFEDTK
1056	54	RhM5103	G	3	IGHV3-SC11	IGHJ5-LC1	5.7%	11	IGLV3-SC4	IGLJ2-2	1.1%	11	VIYEDSE
1534	54	RhM5103	G	3	IGHV3-SC11	IGHJ5-LC1	7.9%	11	IGLV3-SC4	IGLJ2-2	0.7%	11	VIYEDSE
1669	36	RhM46-11	G	4	IGHV4-48	IGHJ5-LC1	8.3%	14	IGLV3-17	IGLJ2-2	4.8%	11	IIYEDNK
1912	36	RhM46-11	G	4	IGHV4-48	IGHJ5-LC1	17.1%	14	IGLV3-17	IGLJ2-2	5.2%	11	IIYEDNK
2552	36	RhM46-11	G	4	IGHV4-48	IGHJ5-LC1	12.4%	14	IGLV3-17	IGLJ2-2	5.2%	11	IIYEDNK
1614	36	RhM46-11	G	4	IGHV4-48	IGHJ5-LC1	11.2%	14	IGLV3-17	IGLJ2-2	5.3%	11	IIYEDNK
1825	62.1	RhM5107	G	5	IGHV4-48	IGHJ4-4	8.0%	13	IGLV3-17	IGLJ2-2	3.1%	11	IIYEDSK
2630	62.1	RhM5107	G	5	IGHV4-48	IGHJ4-4	7.7%	13	IGLV3-17	IGLJ2-2	4.2%	11	IIYEDSK
1410	62.1	RhM5107	G	5	IGHV4-48	IGHJ4-4	7.0%	13	IGLV3-17	IGLJ2-2	3.4%	11	IIYEDTK
1816	62.1	RhM5107	G	5	IGHV4-48	IGHJ4-4	9.1%	13	IGLV3-17	IGLJ2-2	4.5%	11	IIYEDNK
1601	36	RhM46-11	G	6	IGHV4-79	IGHJ4-4	12.3%	12	IGLV3-17	IGLJ1-LC1	3.8%	11	IIYEDNK
1671	36	RhM46-11	G	7	IGHV4-79	IGHJ5-LC1	15.2%	14	IGLV3-17	IGLJ2-2	6.1%	11	IIYEDSK
2212	36	RhM46-11	G	8	IGHV4-79	IGHJ4-4	10.4%	12	IGLV3-17	IGLJ1-LC1	4.5%	11	IVYEDSK
2553	36	RhM46-11	G	9	IGHV4-79	IGHJ5-LC1	13.7%	15	IGLV3-17	IGLJ2-2	6.3%	11	IIYEDSR
1819	62.1	RhM5107	G	10	IGHV4-79	IGHJ5-LC1	11.2%	12	IGLV3-17	IGLJ2-2	4.6%	11	IMYEDTK
975	62.1	RhM5107	G	11	IGHV4-79	IGHJ4-4	8.3%	11	IGLV3-17	IGLJ1-LC1	3.4%	11	IIYEDNK
1447	62.1	RhM5107	G	11	IGHV4-79	IGHJ4-4	9.8%	11	IGLV3-17	IGLJ1-LC1	3.8%	11	IIYEDNK
1823	62.1	RhM5107	G	11	IGHV4-79	IGHJ4-4	8.3%	11	IGLV3-17	IGLJ1-LC1	2.6%	11	IIYEDNK
1824	62.1	RhM5107	G	11	IGHV4-79	IGHJ4-4	7.9%	11	IGLV3-17	IGLJ1-LC1	3.0%	11	TYIEDTK
2201	36	RhM46-11	G	12	IGHV4-96	IGHJ4-4	8.7%	11	IGLV3-17	IGLJ1-LC1	3.8%	11	IIYEDNK
2536	36	RhM46-11	G	13	IGHV4-96	IGHJ5-LC1	8.7%	15	IGLV3-17	IGLJ2-2	6.7%	11	IIYEDSR
2547	36	RhM46-11	G	14	IGHV4-96	IGHJ4-4	11.1%	12	IGLV3-17	IGLJ2-2	4.5%	11	IIYEDSK
2653	36	RhM46-11	G	15	IGHV4-96	IGHJ5-LC1	13.4%	14	IGLV3-17	IGLJ2-2	5.3%	11	IIYEDNK
2548	36	RhM46-11	G	15	IGHV4-96	IGHJ5-LC1	11.8%	14	IGLV3-17	IGLJ2-2	5.9%	11	IIYEDNK
2857	36	RhM46-11	G	16	IGHV2-33	IGHJ4-4	7.7%	10	IGLV1-48	IGLJ1-LC1	10.4%	11	LIYESNK
1809	36	RhM22-11	G	17	IGHV3-108	IGHJ4-4	5.9%	11	IGKV2-118	IGKJ4-LC1	1.5%	9	LIYGGSN
2551	36	RhM46-11	G	18	IGHV3-108	IGHJ4-4	10.7%	14	IGLV1-67	IGLJ2-2	9.4%	11	LIFQNNK
1918	36	RhM46-11	G	19	IGHV3-SC11	IGHJ4-4	14.8%	11	IGKV2-73	IGKJ1-5	1.8%	9	LIYEVSN
2554	36	RhM46-11	G	19	IGHV3-SC11	IGHJ4-4	14.4%	11	IGKV2-73	IGKJ1-5	2.5%	9	LIYEVSN
1806	36	RhM22-11	G	20	IGHV3-SC13	IGHJ4-4	8.4%	5	IGKV2-117	IGKJ1-5	5.9%	9	LIYRASN
2102	62.1	RhM5081	G	21	IGHV3-SC9	IGHJ4-4	4.4%	12	IGLV3-SC6	IGLJ2-2	5.4%	9	VTHKDTE
1510	36	RhM46-11	G	22	IGHV4-100	IGHJ5-LC1	12.8%	18	IGKV1-LC1g	IGKJ4-LC1	6.9%	9	LIFAAAS
2550	36	RhM46-11	G	23	IGHV4-100	IGHJ4-4	10.3%	6	IGLV1-45	IGLJ1-LC1	8.1%	11	LIYNNDR
2847	36	RhM46-11	G	24	IGHV4-100	IGHJ6-6	11.9%	16	IGKV2-118	IGKJ4-LC1	2.6%	9	LIYGGSN
2090	62.1	RhM5081	G	25	IGHV4-97	IGHJ4-4	9.4%	9	IGLV3-SC6	IGLJ2-2	1.6%	9	IYHKDSE
2840	36	RhM46-11	G	26	IGHV5-117	IGHJ4-4	5.6%	13	IGKV2-73	IGKJ4-LC1	4.7%	9	LIYMDSY

1. Mutation frequency reported is an upper-bound estimate given the current incomplete characterization of the rhesus repertoire at the allelic level.

Rows are shaded by study: study #36 (white), study #54 (blue), study #62.1 (gray)

Table S3. Neutralization Data (Related to Table 1)

Antibody	Study	IC50 ($\mu\text{g/ml}$) in TZM-bl Cells ¹					IC50 ($\mu\text{g/ml}$) in A3R5.7 Cells ¹						
		92TH023.6*	MN.3	CM244.c01*	MW965.26*	MLV-SVA	427299.c12	CM244.c01*	254010P00Ra.1	254007P00Ra.1	0503M02138.ec1*	C1080.c03*	C3347.c11*
975	62.1	16.9	>50	>50	>50	>50	>50	>50	>50	>50	>50	>50	>50
1410	62.1	14.5	>50	>50	>50	>50	>50	>50	>50	>50	>50	>50	>50
1447	62.1	17.0	>50	>50	>50	>50	>50	>50	>50	>50	>50	>50	>50
1819	62.1	16.4	>50	>50	>50	>50	>50	>50	>50	>50	>50	>50	>50
1823	62.1	8.9	>50	>50	>50	>50	>50	>50	>50	>50	>50	>50	>50
1824	62.1	6.7	>50	>50	>50	>50	>50	>50	>50	>50	>50	>50	>50
1825	62.1	2.8	>50	>50	>50	>50	>50	>50	>50	>50	>50	>50	>50
1601	36	3.3	>50	>50	>50	>50	>50	>50	>50	>50	>50	>50	>50
1671	36	6.3	>50	>50	>50	>50	>50	>50	>50	>50	>50	>50	>50
1678	36	9.9	>50	>50	>50	>50	>50	>50	>50	>50	>50	>50	>50
1697	36	1.9	>50	>50	>50	>50	>50	>50	>50	>50	>50	>50	>50
1811	36	10.7	>50	>50	>50	>50	>50	>50	>50	>50	>50	>50	>50
2536	36	7.1	>50	>50	>50	>50	>50	>50	>50	>50	>50	>50	>50
2547	36	21.8	>50	>50	>50	>50	>50	>50	>50	>50	>50	>50	>50
2548	36	3.0	>50	>50	>50	>50	>50	>50	>50	>50	>50	>50	>50
2552	36	4.8	>50	>50	>50	>50	>50	>50	>50	>50	>50	>50	>50
2553	36	8.2	>50	>50	>50	>50	>50	>50	>50	>50	>50	>50	>50
2653	36	0.8	>50	>50	>50	>50	>50	>50	>50	>50	>50	>50	41.7
1056	54	>50	>50	>50	18.867	>50	>50	>50	>50	>50	>50	>50	>50
1534	54	>50	>50	>50	14.445	>50	>50	>50	>50	>50	>50	>50	>50
1678_UCA	36	>50	>50	>50	>50	>50	>50	>50	>50	>50	>50	>50	>50
2548_UCA	36	>50	>50	>50	>50	>50	>50	>50	>50	>50	>50	>50	>50
1825_UCA	62.1	>50	>50	>50	>50	>50	>50	>50	>50	>50	>50	>50	>50
1518_ED ²	36	5.2	>50	>50	>50	>50	>50	>50	>50	>50	>50	>50	>50
1518_EA	-	>50	>50	>50	>50	>50	>50	>50	>50	>50	>50	>50	>50
1518_AA	-	>50	>50	>50	>50	>50	>50	>50	>50	>50	>50	>50	>50
CH59 ³	RV144	1.92	>50	>50	>50	>50	>50	>25	>25	>25	>25	>25	>25
CH31 ³	Pos. Control	0.25	0.53	1.34	1.20	>25	0.10	0.02	0.05	0.67	1.83	0.06	0.18

¹Values are the mAb dilution at which relative luminescence units (RLUs) were reduced 50% compared to virus control wells (no test sample).

² 1518_ED = wildtype; 1518_EA = D51A mutant; 1518_AA = E50A+D51A mutant

³ Values for controls include those reported previously (Liao et al 2013)

Values in bold are considered positive for neutralizing antibody when compared against background

Color scale: Red: neutralization at <1 $\mu\text{g/ml}$; orange: <50 $\mu\text{g/ml}$

* Virus has K169 present in V2

Table S4. Candidate Orthologs of Relevant V Gene Segments and Nomenclature Mapping (Related to Fig. 4)

A

VL		
Human	Rhesus	Seq ID%
IGLV3-10	IGLV3-17	96.8
IGLV6-57	IGLV6-92	93.8
IGLV3-22 ^b	IGLV3-30	90.5
VH		
Human	Rhesus	Seq ID%
IGHV3-23	IGHV3-SC11	90.9
IGHV4-59	IGHV4-48	93.5
IGHV4-b	IGHV4-79	92.9
IGHV4-b	IGHV4-96	91.9
IGHV5-51	IGHV5-20	95.2
IGHV3-9	IGHV3-78	93.3

B

Human				Rhesus Ortholog			
RV144 Ab	VH	VL	ED? ^a	NHP Ab	VH	VL	ED? ^a
CH58	IGHV5-51	IGLV6-57	Yes	None	IGHV5-20	IGLV6-92	No
CH59	IGHV3-9	IGLV3-10	Yes	None	IGHV3-78	IGLV3-17	Yes
HG120	IGHV3-23	IGLV3-10	Yes	1678	IGHV3-SC11	IGLV3-17	Yes
None	IGHV4-59	IGLV3-10	Yes	1410	IGHV4-48	IGLV3-17	Yes
None	IGHV4-b	IGLV3-10	Yes	975	IGHV4-79	IGLV3-17	Yes
None	IGHV4-b	IGLV3-10	Yes	2536	IGHV4-96	IGLV3-17	Yes

Table S4. (cont.)**C**

VH		
Rhesus Library	Sundling et al. ^c	Seq ID%
IGHV3-SC11	IGHV3.58	100
IGHV4-48	IGHV4.22	100
IGHV4-79	IGHV4.34	100
IGHV4-96	IGHV4.38	100
IGHV2-33	IGHV2.12	100
IGHV3-108	IGHV3.44	100
IGHV3-SC13	IGHV3.54	100
IGHV3-SC9	IGHV3.15	99.3
IGHV4-100	IGHV4.40	100
IGHV4-97	IGHV4.39	100
IGHV5-117	IGHV5.46	100
IGHV5-20	IGHV5.7	100
IGHV3-78	IGHV3.33	100
VL		
Rhesus Library	Sundling et al. ^c	Seq ID%
IGLV3-17	IGLV3.4	100
IGLV6-92	IGLV6.40	100
IGLV3-30	IGLV3.12	100
IGLV1-48	IGLV1.19	100
IGLV2-118	IGLV2.59	100
IGLV1-67	IGLV1.30	97.3
IGLV1-45	IGLV1.16	100
IGLV2-117	IGLV2.58	100
IGLV3-SC6	IGLV3.45	100
IGKV1-LC1g	IGKV1.27	100
IGKV2-118	IGKV2.59	100
IGKV2-73	IGKV2.38	99.3

a. Columns denote whether rhesus or human VL gene encodes for the LCDR2 ED motif

b. IGLV3-22 has putative dominant non-functional allele (see text for details)

c. Mapping of rhesus repertoire V gene nomenclature described here to nomenclature previously described (Sundling et al. 2012)

Table S5. Data collection and refinement statistics for CH59-UA (Related to Fig 6)

Structure	CH59-UA
Data collection	
Space group:	P2 ₁ ^a
<i>Cell dimensions</i>	
a, b, c (Å):	76.3, 70.8, 107.3
α, β, γ (°):	90.0, 96.8, 90.0
Resolution (Å):	50-2.4 (2.44-2.40)
R _{merge} (%):	9.0 (36.0) ^b
< l/σ>	17.2 (3.1)
Completeness (%):	99.7 (98.4)
Redundancy:	3.6 (3.1)
Refinement	
Total # reflections:	44692
Unique # reflections:	41986
Rwork / Rfree (%):	18.2 / 22.9 (21.2 / 27.1)
Average B factor (Å ²):	35.04
Nonhydrogen atoms ^c :	6369+72 ^d
Water molecules:	204
R.M.S. deviations	
Bond lengths (Å):	0.006
Bond angles (°):	1.068
ψ, φ favored (%):	97.1
ψ, φ allowed (%):	2.8
ψ, φ outlying (%):	0.1

a These crystals had two Fabs in the asymmetric unit.

b Values in parentheses are for the highest resolution shells.

c Not including water molecules.

d Protein atoms, plus 72 organic molecule and ion atoms.

Table S6. Rhesus PCR Primers (Related to Fig. 1)

RT primers	Oligosequence(5' to 3')
RhlG_RTV4	TCTTGTCACCTGGTGTG
RhlM_RTV4	TGAATTCCAGGAGAAAGTGTG
RhlA_RTV4	TGTTCCRGATTTGAGATGGTG
RhlD_RTV4	AAGGTCTCCTGCTTGTATC
RhlE_RTV4	TTGGAATCTGCACACTCTTG
RhCK_RTV6	TCTCTGGGATAGAAGTATTGAG
RhCL_RTV6	CTTGTGTTGCTGTGTTGGAG
RhlG_EXTV5	GAAGAAGCCCTGGACAGCAGGC
RhlG_EXTV5	AAGGTGTGCACGCCGCTGGTCAG
RhlM_EXTV5	GTCGGGAAGGAAGTCTGTGGAGG
RhlD_EXTV5	TCCCCAGGTGCCAGGTGACAGTCAC
RhlE_EXTV5	ACGGTCAGCAAGCTGATGGTGGCA

PCRα Heavy Chain Primers	Oligosequence(5' to 3')
RHIGVH1+7_EXT1	CACCATGGACTGGACCTGGAGGMTCCTC
RHIGVH1+7_EXT2	CACCATGGACCTGACCCGGAGGATCCTTTTC
RHIGVH2_EXT	CACCATGGACACGCTTGTCCACRCTC
RHVH3_EXT1_N	CATGGAGTTgGGGCTGAGCTGGGTTTCC
RHVH3_EXT2_N	CATGGAGTTgGGGCTGAGYTGGGTTTCC
RHVH3_EXT3_N	CATGGAGTTGGGCTGAGCTGGT
RHVH3_EXT4_N	CATGGAGTTGGGCTGAGCTKGTTTYC
RHVH4_EXT1_N	ACCATGAAGCACCTGTGGITCTBCCCTCTCC
RHVH4_EXT2_N	CACCATGAAGCACCTGKGGTTCTY
RHIGVH5_EXT	CACCATGGGGTCAACTGCCMTCTC
RHIGVH6_EXT	CCATGTCTGTCCTCTCATCGTC

PCRα Kappa Chain Primers	Oligosequence(5' to 3')
RhCK_EXTV7	ACCTGTACCTCAGATGGCGGGAAAGATG
RHIGVK1_EXT1_N	CACCATGGACATGAGGGYCCC
RHIGVK1_EXT2_N	CACCATGGACATGAGGGTCCCCAGTC
RHIGVK1_EXT3_N	CACCATGGACATGAGGGTCCCCGGTAIC
RHIGVK1_EXT4_N	CACCATGGACATGAGGGTCYCCGGTCAG
RHIGVK1_EXT5_N	CACCATGGACATGAGGGTCCCCGGTCAGCTYC
RHIGVK2_EXT1_N	CACCATGAGGCTCCWGCTCAG
RHIGVK2_EXT2_N	CACCATGAGGCTCCCTGCTCAGCTYCTGGGC
RHIGVK3_EXT1_N	CACCATGGAAGCCCCAGCTCRGCTTCTC
RHIGVK3_EXT2_N	CACCATGGAAGCCCCAGCACAGCTTCTC
RHIGVK4_EXT	CACCATGGTGTACAGACCCAAGWCTTC
RHIGVK5_EXT	CACCATGGGATCCCAGGTTCACCTCCTCAG
RHIGVK6_EXT1	CACCATGGTGTCCCCATTGCAACTCCTG
RHIGVK6_EXT2	CACCATGTGTCTCCATCACAACATG
RHIGVK7_EXT	CACCATGGGGTCTGGGCTCTTCTG

PCRα Lambda Chain Primers	Oligosequence(5' to 3')
RhCL_EXTV7	TGCCATCTGCCTCCAGGCCACTT
RHIGVL1_EXT1	CACCATGGCCTGGTCTCCTCTCSTCCTCAC
RHIGVL1_EXT2	CACCATGGCCTGGTCTCCTCTCCTCTC
RHIGVL2_EXT	CACCATGGCCTGGGCTGTGCTCCTC
RHIGVL3_EXT1	CACCATGGCGGGGACCCYTCTCCTCCTC
RHIGVL3_EXT2_N	CACCATGGCCTGGACCCCTGTTCTGCTC
RHIGVL3_EXT3	CACCATGGCCTGGACCCCTCCTCTC
RHIGVL4_EXT	CACCATGGCCTGGACCCACTCCTCCTC
RHIGVL5_EXT	CACCATGGCCTGGACTCYTCTC
RHIGVL6_EXT	CACCATGGCCTGGGCTCCACTCCTCCTC
RHIGVL7_EXT	CACCATGGCCTGGACTCTGCTCCTCCTC
RHIGVL8_EXT	CACCATGGCCTGGATGATGCTCCTCCTC
RHIGVL11_EXT	CACCATGGCCCTGACTCCTCCTCCTC

PCRb Heavy Chain Primers	
Oligoname	Oligosequence(5' to 3')
RhlgA_ACD_IntV20	CAGGGCCGCTGTGCTCTCGGAGGTGCTCCCTGCCCTCGAGGCTCAGCGGGAAAGAC
RhlgA_BC_IntV20	CAGGGCCGCTGTGCTCTCGGAGGTGCTCCCTGCAGAGGYTCAGCGGGAAAGAC
RhlgG_IntV20	CAGGGCCGCTGTGCTCTCGGAGGTGCTCCCTGGAG
RhlgM_IntV20	CAGGGCCGCTGTGCTCTCGGAGGTGCTCCCTCACAGGAGACGAGGGGAAAAG
RhlgD_IntV20	CAGGGCCGCTGTGCTCTCGGAGGTGCTCCCTGTTACCTTGGAGTTGGCA <u>G</u> GCTG
RhlgE_IntV20	CAGGGCCGCTGTGCTCTCGGAGGTGCTCCCTGCAGCAGGGATCAAGGGGAAGAC
RHIGVH1+7_INT1	CCAAGCTGGCTAGCACCATTGAGACTGGACCTGGAGGMTCCTC
RHVH1+7_INT2_N	CCAAGCTGGCTAGCACCATTGAGACAGCCTTGCTCCAC
RHIGVH2_INT	CCAAGCTGGCTAGCACCATTGAGTTGGGCTGAGYTG
RHVH3_INT1_N	CCAAGCTGGCTAGCACCATTGAGTTGGGCTGAGCTKG
RHVH3_INT2_N	CCAAGCTGGCTAGCACCATTGAGACACCTGKGGTTC
RHVH4_INT_N	CCAAGCTGGCTAGCACCATTGGGTCACAGCCMTCCCTC
RHIGVH5_INT	CCAAGCTGGCTAGCACCATTGGGTCACAGCCMTCCCTC
RHIGVH6_INT	CCAAGCTGGCTAGCACCATTGCTGTCCTCCTCATCGTC

PCRb Kappa Chain Primers	
Oligoname	Oligosequence(5' to 3')
RhCK_INTv6	TGGCGGGAAGATGAAGACAGATGGT
RHIGVK1_INT1_N	CCAAGCTGGCTAGCACCATTGAGACATGAGGGYCCC
RHIGVK1_INT2_N	CCAAGCTGGCTAGCACCATTGAGACATGAGGGCYCCG
RHIGVK2_INT1_N	CCAAGCTGGCTAGCACCATTGAGGCTCCWGCTC
RHIGVK3_INT1_N	CCAAGCTGGCTAGCACCATTGAGACCCCCAGCWC
RHIGVK4_INT	CCAAGCTGGCTAGCACCATTGAGTCACAGACCCAAG
RHIGVK5_INT	CCAAGCTGGCTAGCACCATTGGATCCCAGGTTACCTCC
RHIGVK6_INT1	CCAAGCTGGCTAGCACCATTGGTGTCCCCATTGCAACTC
RHIGVK6_INT2	CCAAGCTGGCTAGCACCATTGGTGTCCCCATTGCAACTC
RHIGVK7_INT	CCAAGCTGGCTAGCACCATTGGGTCCTGGGCTCCCTTCC

PCRb Lambda Chain Primers	
Oligoname	Oligosequence(5' to 3')
RhCL_INTv6	GTCACTGATCAGACACACTAGTGTGG
RHIGVL1_INT	CCAAGCTGGCTAGCACCATTGCCCTGGCTCCTCTC
RHIGVL2_INT	CCAAGCTGGCTAGCACCATTGCCCTGGGCTCTGSTCC
RHIGVL3_INT1_N	CCAAGCTGGCTAGCACCATTGCCGGGACCCYTC
RHIGVL3_INT2_N	CCAAGCTGGCTAGCACCATTGCCCTGGGACCCCTS
RHIGVL4_INT_N	CCAAGCTGGCTAGCACCATTGCCCTGGGACCCACTCC
RHIGVL5_INT	CCAAGCTGGCTAGCACCATTGCCCTGGACTCYTCTC
RHIGVL6_INT_N	CCAAGCTGGCTAGCACCATTGCCCTGGGCTCCACTC
RHIGVL7_INT	CCAAGCTGGCTAGCACCATTGCCCTGGACTCTGCTCCCTC
RHIGVL8_INT	CCAAGCTGGCTAGCACCATTGCCCTGGATGATGCTCTC
RHIGVL11_INT	CCAAGCTGGCTAGCACCATTGCCCTGACTCCTCTCCTC

Sequencing Primers	
Oligoname	Oligosequence(5' to 3')
RHVHKLSEQ_F	CCAAGCTGGCTAGCACCATTG
RHVHSEQ_R	CTGTGCTCTCGGAGGTGCTC
RHVKSEQ_R	GGAAGATGAAAGACAGATGGTG
RHVLSEQ_R	TGATCAGACACACTAGTGTGG

Supplemental Experimental Procedures

Sequence Analysis

An annotated rhesus repertoire library consisting of VH, DH, JH, VK, JK, V λ and J λ gene segments was used for both rhesus ortholog analysis and inference of VDJ rearrangements. This library was obtained by searching the sequence data for the NCBI *Macaca mulatta* whole genome sequencing project rather than the assembled genome. We used human gene segments as search queries, and examined all retrieved hits for functionality, retaining only those sequences with intact codons for the invariant residues, intact RS sequences, and without stop codons. These sequences were supplemented by sequences obtained from the King's College database (http://www.kcl.ac.uk/immunobiology/Mac_ig/). Duplicate sequences were discarded, and judgments based on similarity were made as to whether sequences were related as alleles or distinct gene segments. Nomenclature of the rhesus V gene segments of this library differ from a previous characterization of the rhesus repertoire (Sundling et al., 2012) and a mapping to the Sundling et al. nomenclature for the relevant V genes observed in this study is provided in Table S4C. The term “ortholog” is used throughout this paper to reflect putative orthology representative of high sequence identity between a pair of genes that belong to a class of genes of shared functionality. Identification of orthology between human and rhesus Ig genes was performed by searching for high sequence identity matches between the rhesus repertoire library and human Ig genes from the IMGT database (Lefranc, 2001). The V(D)J arrangements of rhesus antibodies were inferred using a Bayesian inference method as previously described (Kepler, 2013; Munshaw and Kepler, 2010).

The BLAT web server (Kent, 2002; Kuhn et al., 2013) was used to search for orthologs of human IGLV3-10 in the following primate genomes: *Microcebus murinus* (Lindblad-Toh et al., 2011), *Otolemur garnettii* (OtoGar3 assembly: <http://www.ncbi.nlm.nih.gov/assembly/396188>) (Lindblad-Toh et al., 2011), *Tarsius syrichta* (TarSyr1 assembly: <http://www.ncbi.nlm.nih.gov/assembly/64501>) (Lindblad-Toh et al., 2011), *Callithrix jacchus* (CalJac3 assembly: <http://www.ncbi.nlm.nih.gov/assembly/6608>), *Saimiri boliviensis* (SaiBol1.0 assembly: <http://www.ncbi.nlm.nih.gov/assembly/420378>), *Macaca mulatta* (Gibbs et al., 2007), *Papio anubis* (Panu_2.0 assembly: <http://www.ncbi.nlm.nih.gov/assembly/399268>), *Nomascus leucogenys* (Nleu_3.0 assembly: <http://www.ncbi.nlm.nih.gov/assembly/506498>), *Pongo abelii* (Locke et al., 2011), *Pan troglodytes* (PanTro4 assembly: <http://www.ncbi.nlm.nih.gov/assembly/255628>) (Consortium, 2005), and *Gorilla gorilla* (Scally et al., 2012). In addition, we used BLAST with human IGLV3-10 as the query against the RefSeq genomic database (Pruitt et al., 2014) to search for orthologs in *Pan paniscus* because the genome assembly of *Pan paniscus* (Prufer et al., 2012) was not yet available through the BLAT web server.

Molecular Modeling

Threading was accomplished using the Rosetta protein modeling software package (Leaver-Fay et al., 2011). For the structural model of ab975 in complex with V2, the sequence of ab975 heavy and light chains were threaded independently onto a template of the CH59 structure over 1000 iterations. The top scoring heavy and light chain models were then combined onto the joint template of the CH59 Fab structure in complex with V2. This model was further refined and underwent energy minimization using the AMBER ff03 force field (Case

et al., 2005; Duan et al., 2003). For the structural model of rhesus IGHV3-78 and IGLV3-17, the germline IGHV3-78 sequence was concatenated to the CH59-UA HCDR3 and heavy chain framework 4 sequence and threaded onto a template of the CH59-UA heavy chain structure. Next, the germline IGLV3-17 sequence was concatenated to the CH59-UA LCDR3 and light chain framework 4 sequences and threaded onto a template of the CH59-UA light chain. Threading for each chain was run for 1000 iterations and the top model for each selected and combined onto the joint template of the CH59-UA Fab structure. Lastly the model was superposed onto the CH59-V2 complex and the V2 coordinates transferred thus positioning the V2 peptide in the CH59 binding orientation within the binding site of the IGHV3-78/IGLV3-17 model.

Supplemental References

- Case, D.A., Cheatham, T.E., 3rd, Darden, T., Gohlke, H., Luo, R., Merz, K.M., Jr., Onufriev, A., Simmerling, C., Wang, B., and Woods, R.J. (2005). The Amber biomolecular simulation programs. *J Comput Chem* 26, 1668-1688.
- Consortium, C.S.a.A. (2005). Initial sequence of the chimpanzee genome and comparison with the human genome. *Nature* 437, 69-87.
- Duan, Y., Wu, C., Chowdhury, S., Lee, M.C., Xiong, G., Zhang, W., Yang, R., Cieplak, P., Luo, R., Lee, T., et al. (2003). A point-charge force field for molecular mechanics simulations of proteins based on condensed-phase quantum mechanical calculations. *J Comput Chem* 24, 1999-2012.
- Gibbs, R.A., Rogers, J., Katze, M.G., Bumgarner, R., Weinstock, G.M., Mardis, E.R., Remington, K.A., Strausberg, R.L., Venter, J.C., Wilson, R.K., et al. (2007). Evolutionary and biomedical insights from the rhesus macaque genome. *Science* 316, 222-234.
- Kent, W.J. (2002). BLAT--the BLAST-like alignment tool. *Genome Res* 12, 656-664.
- Kepler, T.B. (2013). Reconstructing a B-cell clonal lineage. I. Statistical inference of unobserved ancestors. *F1000Res* 2, 103.
- Kuhn, R.M., Haussler, D., and Kent, W.J. (2013). The UCSC genome browser and associated tools. *Brief Bioinform* 14, 144-161.
- Leaver-Fay, A., Tyka, M., Lewis, S.M., Lange, O.F., Thompson, J., Jacak, R., Kaufman, K., Renfrew, P.D., Smith, C.A., Sheffler, W., et al. (2011). ROSETTA3: an object-oriented software suite for the simulation and design of macromolecules. *Methods Enzymol* 487, 545-574.
- Lefranc, M.P. (2001). IMGT, the international ImMunoGeneTics database. *Nucleic Acids Res* 29, 207-209.
- Lindblad-Toh, K., Garber, M., Zuk, O., Lin, M.F., Parker, B.J., Washietl, S., Kheradpour, P., Ernst, J., Jordan, G., Mauceli, E., et al. (2011). A high-resolution map of human evolutionary constraint using 29 mammals. *Nature* 478, 476-482.

- Locke, D.P., Hillier, L.W., Warren, W.C., Worley, K.C., Nazareth, L.V., Muzny, D.M., Yang, S.P., Wang, Z., Chinwalla, A.T., Minx, P., *et al.* (2011). Comparative and demographic analysis of orang-utan genomes. *Nature* **469**, 529-533.
- Munshaw, S., and Kepler, T.B. (2010). SoDA2: a Hidden Markov Model approach for identification of immunoglobulin rearrangements. *Bioinformatics* **26**, 867-872.
- Prufer, K., Munch, K., Hellmann, I., Akagi, K., Miller, J.R., Walenz, B., Koren, S., Sutton, G., Kodira, C., Winer, R., *et al.* (2012). The bonobo genome compared with the chimpanzee and human genomes. *Nature* **486**, 527-531.
- Pruitt, K.D., Brown, G.R., Hiatt, S.M., Thibaud-Nissen, F., Astashyn, A., Ermolaeva, O., Farrell, C.M., Hart, J., Landrum, M.J., McGarvey, K.M., *et al.* (2014). RefSeq: an update on mammalian reference sequences. *Nucleic Acids Res* **42**, D756-763.
- Scally, A., Dutheil, J.Y., Hillier, L.W., Jordan, G.E., Goodhead, I., Herrero, J., Hobolth, A., Lappalainen, T., Mailund, T., Marques-Bonet, T., *et al.* (2012). Insights into hominid evolution from the gorilla genome sequence. *Nature* **483**, 169-175.
- Sundling, C., Li, Y., Huynh, N., Poulsen, C., Wilson, R., O'Dell, S., Feng, Y., Mascola, J.R., Wyatt, R.T., and Karlsson Hedestam, G.B. (2012). High-resolution definition of vaccine-elicited B cell responses against the HIV primary receptor binding site. *Sci Transl Med* **4**, 142ra196.